

Anomalous Spin Polarization of GaAs Two-Dimensional Hole Systems

R. Winkler,^{1,2} E. Tutuc,² S. J. Papadakis,² S. Melinte,² M. Shayegan,² D. Wasserman,² and S. A. Lyon²

¹*Institut für Festkörperphysik, Universität Hannover, Appelstr. 2, D-30167 Hannover, Germany*

²*Department of Electrical Engineering, Princeton University, Princeton, NJ 08544*

(Dated: February 24, 2019)

We report measurements and calculations of the spin-subband depopulation, induced by a parallel magnetic field, of dilute GaAs two-dimensional (2D) hole systems. The results reveal that the shape of the confining potential dramatically affects the values of in-plane magnetic field at which the upper spin subband is depopulated. Most surprisingly, unlike 2D electron systems, the carrier-carrier interaction in 2D hole systems does not significantly enhance the Zeeman splitting. We interpret our findings using a multipole expansion of the spin density matrix, and suggest that the suppression of the enhancement is related to the holes' band structure and effective spin $j = 3/2$.

PACS numbers: 73.50.-h, 71.70.Ej, 73.43.Qt

It was first pointed out by Janak that for a two-dimensional electron system (2DES) in a static magnetic field the exchange interaction acts like an effective magnetic field (in addition to the applied field) so that the Zeeman energy splitting is enhanced [1]. Recently, the Zeeman splitting of interacting 2D carrier systems has been a subject of renewed interest [2, 3, 4, 5, 6, 7, 8, 9, 10, 11, 12, 13, 14, 15, 16, 17, 18], fueled by the promise of a paramagnetic to ferromagnetic ground state transition at very low densities [19, 20], and the possibility that the spin polarization is related to the apparent metal-insulator transition in dilute 2D systems [21]. Experiments have mostly focused on determining the spin susceptibility from magneto-transport [2, 3, 4, 5, 6, 7, 8, 9], and magnetization [10] measurements. The results generally show that the spin susceptibility of 2DESs in different materials, e.g., Si [2, 3, 4, 5, 10], GaAs [6, 7], and AlAs [8, 9] increases as the density is reduced, one report [3] even suggesting a ferromagnetic instability at the lowest densities.

Lately, the spin polarization of GaAs 2D *hole* systems (2DHSs) has become the subject of intensive research [11, 12, 13, 14, 15, 16, 17] because the holes have a larger effective mass (than electrons) so that they can be made effectively more dilute while maintaining high quality. Furthermore, the spin polarization of holes is important in the context of ferromagnetic semiconductors such as GaMnAs where it is known that the ferromagnetism is mediated by the itinerant valence band holes [22, 23]. We show here that the spin polarization of 2DHSs depends dramatically on the shape of the confining potential. Moreover, even in very dilute 2DHSs we find no significant enhancement of the measured Zeeman splitting as compared with calculations which neglect exchange-correlation. We will argue that this surprising behavior is related to the holes' band structure and effective spin $j = 3/2$ rather than $j = 1/2$ which is the case for electrons.

Four samples from different wafers, including two GaAs/AlGaAs heterojunctions and two GaAs quantum

TABLE I: Typical densities n (in 10^{10} cm^{-2}) and mobilities μ (in m^2/Vs) of the samples used in this study.

sample	carriers	structure	substrate	n	μ
H	holes	heterojunction	(001)	5.3	30
Q1	holes	150 Å wide QW	(001)	4.8	11
Q2	holes	200 Å wide QW	(113)A	6.8	55 [†]
A	electrons	heterojunction	(001)	3.0	48

[†] μ for $\mathbf{I} \parallel [3\bar{3}\bar{2}]$. For $\mathbf{I} \parallel [\bar{1}10]$ we have $\mu = 35 \text{ m}^2/\text{Vs}$.

wells (QWs) flanked by AlGaAs barriers, were investigated in this study (Table I). Depending on their substrate orientation and carrier type, our samples were either Be-doped (samples H, Q1) or Si-doped (Q2, A). All samples were fitted with metal front and back gates to control their density as well as the electric field perpendicular to the 2D systems. We made measurements in ³He or dilution refrigerators down to a temperature $T = 0.03 \text{ K}$ and in magnetic fields up to 25 T.

In Fig. 1(a) we show the longitudinal resistivity ρ_{xx} versus in-plane magnetic field B_{\parallel} for samples H and Q1 both measured at a density of $n = 3.7 \times 10^{10} \text{ cm}^{-2}$. The data shows a positive magnetoresistance with a marked change in functional form above the magnetic field B_d that reflects the complete depopulation of the minority spin subband [2, 15]. In Fig. 1(a) B_d is marked by arrows. Remarkably, the field B_d depends greatly on the shape of the confining potential. Indeed, we have $B_d \simeq 10.6 \text{ T}$ for sample H and $B_d \simeq 20.5 \text{ T}$ for sample Q1, even though the data were taken at the *same* density. In Fig. 1(c) we show B_d in sample H when the electric field \mathcal{E} across the junction is varied by means of front and back gates such that n is kept constant at $4.5 \times 10^{10} \text{ cm}^{-2}$. The field B_d increases significantly with increasing \mathcal{E} . In Fig. 2(a) we show the measured B_d versus n for sample H. The values of B_d depend rather sensitively on whether n is changed by means of a front or back gate.

In order to explain the experimental results of Figs. 1 and 2 we have performed parameter-free calculations

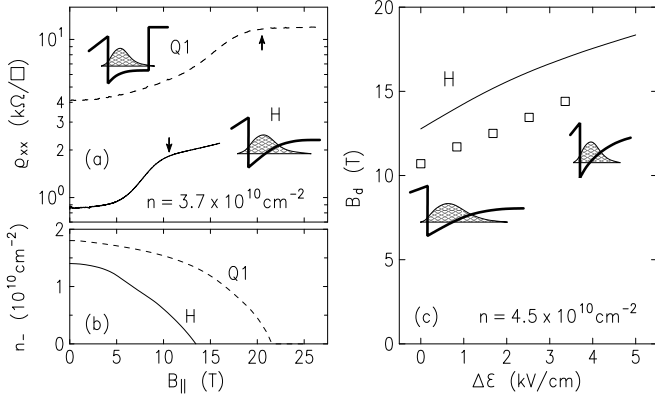


FIG. 1: (a) Longitudinal resistivity ρ_{xx} versus in-plane magnetic field $B_{||}$ measured at $T = 0.3$ K for 2D hole samples, H and Q1, at the same density $n = 3.7 \times 10^{10} \text{ cm}^{-2}$. The depopulation fields B_d are marked by arrows. (b) Calculated density n_- in the minority spin subband of samples H and Q1 as a function of $B_{||}$. (c) Measured (squares) and calculated (solid line) depopulation field B_d versus change $\Delta\mathcal{E}$ of the electric field in sample H for constant density $n = 4.5 \times 10^{10} \text{ cm}^{-2}$.

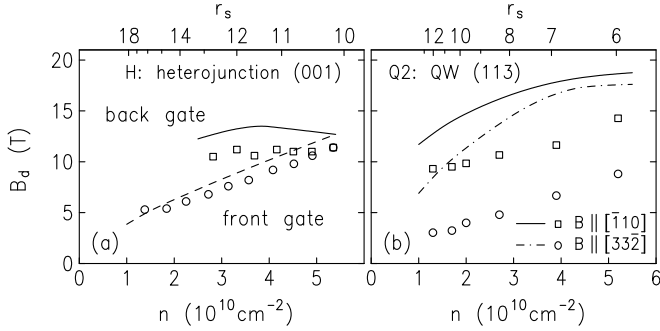


FIG. 2: Measured (symbols) and calculated (lines) depopulation field B_d as a function of n for samples (a) H and (b) Q2. In (a), for the solid line and squares (dashed line and circles) n was varied via a back (front) gate. In (b) the different symbols refer to $\mathbf{B} \parallel [110]$ and $\mathbf{B} \parallel [332]$ as indicated. The upper horizontal axes show the calculated density parameter r_s for the corresponding n . In (a) we used $r_s(n)$ for the front gate.

in the multiband envelope-function and self-consistent Hartree approximations and taking into account the effect of finite-layer thickness [7, 24]. Figure 1(b) shows the calculated density n_- in the minority spin subband as a function of $B_{||}$. The lines in Figs. 1(c) and 2 show the calculated B_d for the corresponding experiments [25]. The calculations reproduce the different behavior of samples H and Q1 in satisfactory agreement with experiment.

The surprising dependence of the measured B_d on the shape of the confining potential is due to the fact that hole states have an effective spin $3/2$ [24]. Subband quantization in 2DHSs yields a quantization of angular momentum $m = \pm 3/2$ for the heavy holes (HHs) and $m = \pm 1/2$ for the light holes (LHs). The quantization axis of angular momentum that is enforced by HH-LH

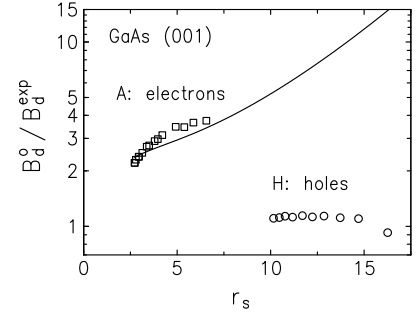


FIG. 3: Ratio B_d^0/B_d^{exp} of the depopulation field B_d^0 calculated neglecting exchange-correlation to the measured field B_d^{exp} for a 2DES (squares) and a 2DHS (circles) in GaAs (001) heterojunctions plotted versus the density parameter r_s . In both cases, n was varied via a front gate. For electrons, the solid line shows the ratio B_d^0/B_d^{xc} , where B_d^{xc} was calculated taking into account exchange-correlation [7, 29].

splitting points perpendicular to the 2D plane. The Zeeman energy splitting due to $B_{||}$ thus competes with the HH-LH splitting. Since a strong orbital confinement increases the HH-LH splitting we get a reduced Zeeman energy splitting (i.e., a larger B_d), as seen in our experiments [26, 27].

A most remarkable aspect of the results in Figs. 1 and 2(a) is the reasonable *quantitative* agreement between the experimental data and the calculations. This is particularly puzzling because many-particle effects beyond the Hartree approximation (i.e., exchange-correlation effects) were not taken into account. This is in sharp contrast to the case of dilute 2DESs for which it is known that exchange-correlation significantly increases the Zeeman splitting when n is reduced [1, 18, 28, 29, 30]. To quantify this point we show in Fig. 3 the ratio B_d^0/B_d^{exp} of the depopulation field B_d^0 , calculated neglecting exchange-correlation, to the measured field B_d^{exp} for a 2DES (squares) [31] and the 2DHS (circles) in sample H. The ratio thus reflects the enhancement of the Zeeman splitting due to exchange-correlation. Our results are plotted as a function of the dimensionless density parameter r_s defined as the average interparticle spacing measured in units of the effective Bohr radius a_B^* , $r_s \equiv 1/(a_B^* \sqrt{\pi n})$.

For the 2DES in Fig. 3 the ratio B_d^0/B_d^{exp} is between 2 and 4 and, as expected, it increases with r_s . We also remark that for electrons the experimentally observed reduction of B_d is in reasonable quantitative agreement with numerical calculations that take exchange-correlation into account. To illustrate this point, the solid line in Fig. 3 shows the ratio B_d^0/B_d^{xc} , where B_d^{xc} was calculated in the framework of spin-density-functional theory using a parameterization of the polarization-dependent exchange-correlation potential that was recently obtained by means of quantum Monte Carlo calculations [7, 29]. For the 2DHS, on the other hand,

the expected enhancement of the Zeeman splitting and B_d^0/B_d^{exp} ratio is conspicuously absent in Fig. 3. Note that, because of their larger effective mass compared to GaAs electrons ($m^* \simeq 0.25$ compared to $m^* = 0.067$; here m^* is given in units of the free-electron mass), 2DHSs have significantly larger r_s and are thus effectively much more dilute. Nonetheless, the ratio B_d^0/B_d^{exp} remains close to unity up to the largest values of r_s where a greater than ten-fold enhancement is expected.

Before discussing possible reasons for this anomalous behavior of 2DHSs, we make remarks regarding the effective mass m^* which enters a_B^* and thus determines r_s . For holes, m^* is not uniquely defined. First, the HH dispersions are typically nonparabolic, meaning that m^* depends on energy and therefore on n and the confinement potential. Second, the HH systems have a large Rashba and Dresselhaus spin splitting at $B = 0$ [24], leading to two energy versus wavevector (\mathbf{k}_{\parallel}) dispersions with different curvatures and effective masses m_+^* and m_-^* . Commonly, values of m^* between about 0.2 and 0.4 are used for holes in GaAs [11, 12, 13, 24, 32]. Here we adopt a simple definition for an average effective mass $\langle m^* \rangle$:

$$\langle m^* \rangle = \hbar^2 \pi n / (2 \langle E_k \rangle), \quad (1)$$

where $\langle E_k \rangle$ is the mean kinetic energy per particle. Note that for a single, parabolic dispersion with an effective mass m^* , the mass $\langle m^* \rangle$ as defined in Eq. (1) properly reduces to m^* and is independent of n . For the 2DHS, on the other hand, $\langle m^* \rangle$ in general depends sensitively not only on n but also on the system's parameters such as the thickness of the 2DHS and on the applied electric and magnetic fields. Figure 4(a) shows the calculated density parameter r_s in sample H, when n is changed by means of a front or back gate. We emphasize that the main conclusion of our work, namely the lack of enhancement of the Zeeman splitting with increasing diluteness, is not affected by the specific values of m^* used to define r_s : it is clear in Fig. 3 that if r_s were changed by a factor of 2 or 3, there would still exist a large discrepancy between the experimental hole data and the expected enhancement. If we take into account Rashba and Dresselhaus spin splitting [24], then we get, similar to Eq. (1), effective masses $\langle m_{\pm}^* \rangle$ for each spin subband. To illustrate this effect, we show $\langle m_{\pm}^* \rangle$ for sample H in Fig. 4(b).

Why do dilute 2DHSs *not* show a significant enhancement of the Zeeman splitting? Using a recently developed multipole expansion of the spin density matrix [17] we argue in the remainder of this paper that the $j = 3/2$ hole spin is the likely culprit. For 2DESs with spin 1/2 it is well-known that the mean Coulomb energy $\langle E_c \rangle$ per particle can be completely characterized using n and (the magnitude of) the spin polarization ζ as independent parameters [28]. This is because the 2×2 spin density matrix of spin 1/2 systems can be decomposed into four independent terms: n (a monopole) and the spin polar-

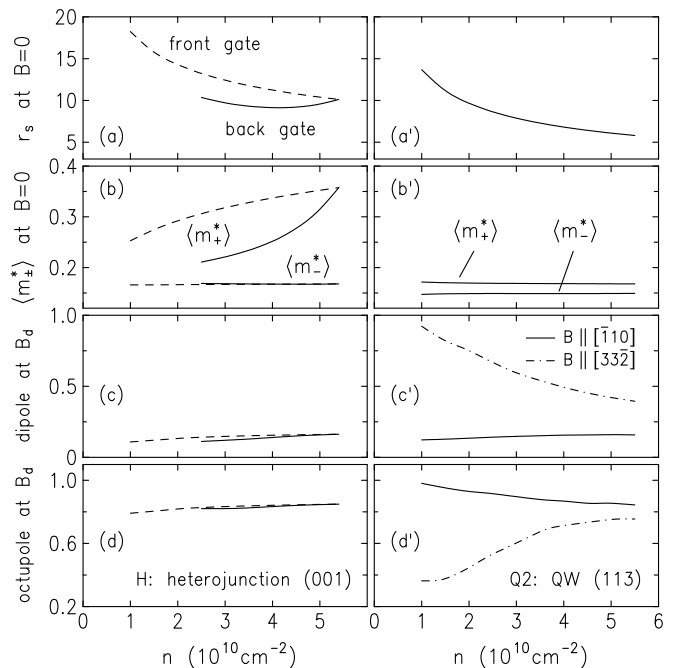


FIG. 4: Calculated density parameter r_s , average effective mass $\langle m_{\pm}^* \rangle$, normalized dipole and octupole moments [33] versus n for samples H and Q2. Line styles have the same meaning as in Fig. 2.

ization vector ζ (a dipole) [17]. In the Hartree-Fock (HF) approximation, the direct part of the Coulomb energy $\langle E_c^{\text{HF}} \rangle$ cancels the potential of the positive background so that only the exchange term $\langle E_x \rangle$ remains [34],

$$\langle E_c^{\text{HF}} \rangle = \langle E_x \rangle = -\frac{2e^2}{3\pi} \sqrt{2\pi n} \left[(1 + \zeta)^{3/2} + (1 - \zeta)^{3/2} \right]. \quad (2)$$

The Coulomb energy $\langle E_c^{\text{HF}} \rangle$ is thus proportional to \sqrt{n} . Higher order terms in a series expansion for $\langle E_c \rangle(n, \zeta)$ of 2DESs were calculated in Ref. [28]. $\langle E_c \rangle$ was calculated numerically in, e.g., Refs. [29, 30].

The 4×4 spin density matrix of $j = 3/2$ 2DHSs, on the other hand, can be decomposed into four multipoles where the monopole is the density n , the dipole corresponds to the spin polarization at $B > 0$, the quadrupole reflects the HH-LH splitting and the octupole is a unique feature of $j = 3/2$ hole systems at $B > 0$ [35]. For sample H, the normalized dipole and octupole at B_d are shown in Figs. 4(c) and (d) [33]. The quadrupole is always close to unity [17] and is not shown in Fig. 4. By definition, these four multipoles provide a set of *independent* parameters that can be used to parameterize the Coulomb energy $\langle E_c \rangle$ of spin 3/2 systems, similar to $\langle E_c \rangle(n, \zeta)$ in spin 1/2 systems [36]. However, the series expansion is presently not known and its calculation represents a formidable task. Our study indicates that the series expansion of $\langle E_c \rangle$ of spin 3/2 2DHSs is qualitatively different from $\langle E_c \rangle(n, \zeta)$ of spin 1/2 2DESs.

The HF exchange energy $\langle E_x \rangle$ of 2D HH systems at

$B = 0$ is the same as $\langle E_x \rangle$ of spin 1/2 2DESs because Eq. (2) requires only that the eigenstates of the two spin subbands for the same \mathbf{k}_{\parallel} are orthogonal [34]. For a HH system, the main effect of a perpendicular magnetic field B_{\perp} is a spin polarization (a dipole), whereas an in-plane field B_{\parallel} usually gives rise to an octupole moment [17, 35]. The spin density matrices at $B_{\perp} > 0$ and $B_{\parallel} > 0$ are thus qualitatively different. However, the HF exchange energy does not distinguish between these cases and always leads to the same enhancement of the exchange energy as in 2DESs. We note that different results for $\langle E_c \rangle$ are obtained in higher-order perturbation theory when the more complicated energy dispersion must be taken into account. This is the reason why the well-established results for exchange-correlation in dilute spin 1/2 2DESs cannot easily be transferred to spin 3/2 2DHSs.

We extend our investigation by comparing the results for sample H with the data for Q2, a QW grown on a (113)A GaAs substrate. Figure 2(b) shows B_d versus n for Q2. The field B_d strongly depends on whether \mathbf{B}_{\parallel} is applied in the in-plane crystallographic directions $[\bar{1}10]$ or $[3\bar{3}\bar{2}]$. The right column of Fig. 4 shows r_s , $\langle m_{\pm}^* \rangle$, the dipole and the octupole moments calculated for Q2. For this sample, when \mathbf{B}_{\parallel} is applied parallel to $[3\bar{3}\bar{2}]$, the measured B_d is well below the calculated value. It is remarkable that for this particular geometry, the octupole remains small, but the 2DHS develops a large dipole moment [Figs. 4(c') and (d')], similar to 2DESs in a \mathbf{B}_{\parallel} . This observation suggests that the Zeeman splitting is enhanced by many-particle effects only when the magnetic field gives rise to a spin polarization. On the other hand, Figs. 2 and 4 suggest that there is no significant enhancement in $j = 3/2$ 2DHSs with a large octupole but a small dipole moment.

Our findings have important implications for the quantum phase diagram of dilute 2DHSs. In dilute *electron* systems, the exchange-correlation enhancement of the Zeeman splitting can be considered a precursor for the ferromagnetic liquid which is expected to be the ground state of ultra-low density 2DESs with $r_s \gtrsim 26$ [29]. The extra multipoles of 2DHSs provide new possibilities for the ground state of hole systems leading to a richer phase diagram than in spin 1/2 electron systems. However, our results suggest that a ferromagnetic phase (i.e., a fully spin-polarized phase with a maximum dipole moment) is often not favored in dilute 2DHSs. This could also have important implications for ferromagnetic semiconductors such as GaMnAs where it is known that the ferromagnetism is mediated by the itinerant spin 3/2 holes in the valence band [22, 23]. In itinerant ferromagnets it is the polarization-dependent competition between the Coulomb energy and the kinetic energy of the interacting carriers which controls the ferromagnetic transition.

We thank BMBF, DOE, NSF, and ARO for support, and D. C. Tsui for illuminating discussions. Part of this work was done at NHMFL; we thank G. Armstrong, T.

Murphy and E. Palm for support.

-
- [1] J. F. Janak, Phys. Rev. **178**, 1416 (1969).
 - [2] T. Okamoto, et al., Phys. Rev. Lett. **82**, 3875 (1999).
 - [3] S. A. Vitkalov, et al., Phys. Rev. Lett. **87**, 086401 (2001).
 - [4] V. M. Pudalov, et al., Phys. Rev. Lett. **88**, 196404 (2002).
 - [5] A. A. Shashkin, et al., Phys. Rev. Lett. **87**, 086801 (2001).
 - [6] J. Zhu, et al., Phys. Rev. Lett. **90**, 056805 (2003).
 - [7] E. Tutuc, et al., Phys. Rev. B **67**, 241309(R) (2003).
 - [8] Y. P. Shkolnikov, et al., Phys. Rev. Lett. **92**, 246804 (2004).
 - [9] K. Vakili, et al., Phys. Rev. Lett. **92**, 226401 (2004).
 - [10] O. Prus, et al., Phys. Rev. B **67**, 205407 (2003).
 - [11] J. Yoon, et al., Phys. Rev. Lett. **82**, 1744 (1999).
 - [12] Y. Y. Proskuryakov, et al., Phys. Rev. Lett. **89**, 076406 (2002).
 - [13] H. Noh, et al., Phys. Rev. B **68**, 165308 (2003).
 - [14] S. J. Papadakis, et al., Phys. Rev. Lett. **84**, 5592 (2000).
 - [15] E. Tutuc, et al., Phys. Rev. Lett. **86**, 2858 (2001).
 - [16] R. Winkler, cond-mat/0401067 (2004).
 - [17] R. Winkler, Phys. Rev. B **70**, 125301 (2004).
 - [18] Y. Zhang and S. Das Sarma, cond-mat/0408335 v2.
 - [19] F. Bloch, Z. Phys. **57**, 545 (1929).
 - [20] E. C. Stoner, Proc. R. Soc. Lond. A **165**, 372 (1938).
 - [21] E. Abrahams, S. V. Kravchenko, and M. P. Sarachik, Rev. Mod. Phys. **73**, 251 (2001).
 - [22] T. Dietl, H. Ohno, and F. Matsukura, Phys. Rev. B **63**, 195205 (2001).
 - [23] M. Abolfath, et al., Phys. Rev. B **63**, 054418 (2001).
 - [24] R. Winkler, *Spin-Orbit Coupling Effects in Two-Dimensional Electron and Hole Systems* (Springer, Berlin, 2003), and references therein.
 - [25] In the calculations, front and back gate are modeled by different boundary conditions for the Hartree potential.
 - [26] The suppression of the Zeeman splitting of 2DHSs has previously been reported in optical [H. W. van Kesteren et al., Phys. Rev. B **41**, 5283 (1990)] and transport [S. Y. Lin et al., Phys. Rev. B **43**, 12110 (1991)] experiments.
 - [27] In Fig. 2(a), the calculated splitting at $B = 0$ between the lowest HH and the lowest LH subband increases from 0.8 to 1.9 meV (decreases from 3.7 to 1.9 meV) when n is increased by means of a front (back) gate [25].
 - [28] A. K. Rajagopal and J. C. Kimball, Phys. Rev. B **15**, 2819 (1977).
 - [29] C. Attacalite, et al., Phys. Rev. Lett. **88**, 256601 (2002).
 - [30] B. Tanatar and D. M. Ceperley, Phys. Rev. B **39**, 5005 (1989).
 - [31] Electron data in Fig. 3 are from sample A of Ref. [7].
 - [32] W. Pan, et al., Appl. Phys. Lett. **83**, 3519 (2003).
 - [33] The multipoles are normalized such that the largest possible values are unity.
 - [34] C. Kittel, *Quantum Theory of Solids* (Wiley, NewYork, 1963); F. Stern, Phys. Rev. Lett. **30**, 278 (1973).
 - [35] Calculations for model HH systems at $B > 0$ (unpublished) suggest that we can have either a large dipole or a large octupole moment, consistent with Fig. 4.
 - [36] Similarly, a Fermi liquid theory for spin 3/2 particles depends on additional independent Fermi liquid parameters beyond those in the usual theory for spin 1/2 systems.